Applied Catalysis B: Environmental 95 (2010) 120–129

Contents lists available at ScienceDirect

Applied Catalysis B: Environmental

journal homepage: www.elsevier.com/locate/apcatb

Catalytic degradation of Orange II in a ferrioxalate-assisted photo-Fenton process using a combined UV-A/C–solar pilot-plant system

J.M. Monteagudo *, A. Durán, I. San Martín, M. Aguirre

University of Castilla-La Mancha, Grupo IMAES, Department of Chemical Engineering, Escuela Técnica Superior de Ingenieros Industriales, Avda. Camilo José Cela, 1, 13071 Ciudad Real, Spain

ARTICLE INFO

Article history:
Received 2 November 2009
Received in revised form 11 December 2009
Accepted 17 December 2009
Available online 24 December 2009

Keywords:
Orange II
Ferrioxalate
Photo-Fenton
Neural networks
CPC

ABSTRACT

The catalytic degradation of Orange II in a ferrioxalate-assisted photo-Fenton process with combined solar and artificial ultraviolet light sources and continuous addition of H_2O_2 was investigated. The reaction was carried out in a pilot plant consisting of a compound parabolic collector (CPC) solar reactor in series with a UV-A/C reactor. An optimization study was done using a multivariate experimental design including the following variables: pH, H_2O_2 flow rate, UV-lamp exposure time, average temperature, average solar power and initial concentrations of Fe(II) and oxalic acid. The photocatalytic degradation efficiency was determined by the analysis of color and total organic carbon (TOC) removal. Under the optimum conditions, TOC removal increased to 99% in only 45 min, and this system permitted the use of a low ferrous concentration of only 2 mg L^{-1}. In addition, oxalic acid was used for pH adjustment. Thus, the operating costs of Fe removal, chemicals and electric power were reduced. Artificial UV-A/C light can be used either to increase the efficiency of the single-solar process or as an alternative to solar CPC on cloudy days. The overall rate constant was split into three components: direct oxidation by hydrogen peroxide, photolytic breakdown of dye–oxalate complexes chromophore group and oxidation by hydroxyl radicals. The influence of the Fe catalyst on the molecular and/or radical reactions was studied by conducting the reaction in the presence and absence of tert-butyl alcohol; the radical mechanism's contribution to the overall degradation increased with increasing iron levels.

1. Introduction

Wastewater from the textile industry contains significant concentrations of organic matter that contribute to the toxicity of the effluents. It is well known that the stability and high degree of aromaticity in azo dyes prevent mineralization of these compounds by conventional aerobic biological treatment processes. Thus, there is currently considerable interest in developing alternative techniques that can degrade organic pollutants and be more cost-effective and environmentally benign [1–3].

The homogenous solar photo-Fenton reaction is one of the most environmentally friendly and economical systems for generating hydroxyl radicals, •OH, and for degrading dye solutions, as previously reported [4,5].

Because H_2O_2 has a maximum absorption at 220 nm and can only absorb photons below 320 nm, ferrioxalate could be used to increase the oxidation efficiency of the solar photo-Fenton process as it is a photo-sensitive complex that is able to expand the useful range of the solar spectrum up to 450 nm [6–9].

Additionally, the photolysis of ferrioxalate generates more H_2O_2 which, with Fe(II), yields more •OH radicals through the well-known Fenton reaction mechanism [10,11], improving the degradation process.

In recent years, ferrioxalate has been used in the photo-Fenton reaction involving ferric compounds, but there is very little information on the ferrioxalate-assisted photo-Fenton system using ferrous-initiated process. The use of ferrous sulfate is advantageous since it is less corrosive that ferric salts, inexpensive and more soluble than ferric compounds. Besides, Fe(II) is quickly converted into Fe(III) in the presence of hydrogen peroxide, so that the destruction of Orange II is basically a process catalyzed by Fe(III)-oxalate.

The degradation of Orange II solutions with sunlight has been previously studied by the authors using the homogeneous catalyst Fe(II) with the addition of H_2O_2 at the beginning of the reaction in the presence of oxalic acid to form ferrioxalate complexes [12] and under a ferrioxalate-assisted solar photo-Fenton process with continuous H_2O_2 addition and air injection during the reaction [13]. Both systems achieved 100% color removal, but lower irradiation times were needed when a continuous dosage of hydrogen peroxide was used. Regarding mineralization, the efficiency of total organic carbon (TOC) removal was higher in

* Corresponding author. Tel.: +34 926295300x3888; fax: +34 926295361.
E-mail address: josemaria.monteagudo@uclm.es (J.M. Monteagudo).

0926-3373/$ – see front matter © 2009 Elsevier B.V. All rights reserved.
doi:10.1016/j.apcatb.2009.12.018

the process with continuous hydrogen peroxide addition (95% vs. 80% hydrogen peroxide addition only at the beginning) because the H_2O_2 scavenger effect was minimized. On the other hand, solar photo-Fenton degradation with oxalic acid is efficient and permits the use of a Fe(II) concentration of only 2 mg L^{-1} and does not require supplemental air injection. Oxalic acid can also be used for pH adjustment, so the operating costs of Fe removal, chemicals and manpower are reduced.

A drawback of this system is that the reaction times on cloudy days are longer. To overcome this disadvantage, the combination (in series) of an artificial UV-A/C pilot plant and a solar-CPC pilot plant was studied in this work.

A multivariate experimental design according to a response-surface methodology [14] was performed to study the effect of all the variables simultaneously (pH, H_2O_2 flow rate, UV-A/C-lamp exposure time (UVL) and initial concentrations of Fe(II) and oxalic acid). The experimental results were fitted using neural networks (NNs) [15,16], which allowed the values of the degradation rate constant (response function) to be estimated within the studied range as a function of the process variables. Additionally, the saliency analysis of each variable in the NNs helped to discern the real relevance of all of them. The decreases of color, TOC and remaining H_2O_2 concentration were monitored. Finally, a kinetic study was also performed on color and TOC removal, and the contributions of direct reaction with H_2O_2, photolytic breakdown in the chromophore group of dye–oxalate complexes and radical reactions on the overall reaction were quantified. The catalytic behavior of Fe and the effects of UV-A or UV-C irradiation were also evaluated.

2. Experimental

2.1. Materials

Orange II solutions were prepared by dissolving Orange II (Aldrich, disodium salt, dye content 85%) in distilled water, without further purification. $FeSO_4{\cdot}7H_2O$ (Panreac, analytical grade) and $H_2C_2O_4{\cdot}2H_2O$ (Panreac, 99.5%) were added to the wastewater to form ferrioxalate complexes and used immediately in situ because of their light sensitivity. The initial concentration of dye was always 20 mg L^{-1}.

In all experiments, after addition of Fe(II) and oxalic acid and pH adjustment an initial amount (~8 mL) of commercial hydrogen peroxide (30%, w/v, Merck) was added to the reactor to bring the H_2O_2 initial concentration to 75 mg L^{-1} at the beginning of the reaction. During the reaction, H_2O_2 was added through a needle (inner diameter 3 mm) at a selected constant flow rate (between 0 and 1 mL min^{-1}) by means of a precision syringe pump (Terumo, model STC-521) coupled with a 60 mL syringe. The needle extended 70 cm into the reactor with the tip immersed in the liquid. By the end of the experiment, between 45 and 50 mL of hydrogen peroxide solution had been added to the reactor. The small addition of H_2O_2 solution and the periodic removal of solution samples did not significantly change the volume of the reaction mixture (50 L). Solutions, 0.1 M H_2SO_4 and 6 M NaOH, were used for pH adjustment of the dye solutions prior to degradation. To evaluate the contribution of the breakdown of dye–oxalate complex chromophore groups to overall degradation, the reaction was carried out with irradiation of the dye solution in the presence of oxalic acid only, using combined solar–UV-A/C light. To quantify the oxidation levels by radical reactions, the scavenging of hydroxyl radicals was accomplished with tert-butyl alcohol. Before analysis, all the samples were withdrawn from the reactor and immediately treated with excess Na_2SO_3 solution to prevent further oxidation (this procedure was tested in order to prevent an overestimation of the degradation).

2.2. Photochemical reactions

2.2.1. Solar-CPC pilot plant

The CPC plant (manufactured by Ecosystem, S.A.) comprised a solar reactor consisting of a continuously stirred tank (52 L), a centrifugal recirculation pump, a solar collector unit with an area of 2 m^2 (concentration factor = 1) and connecting tubing and valves, all in an aluminum frame mounted on a fixed, south-facing platform tilted at 45° in Ciudad Real, Spain (Fig. 1). The total illuminated volume inside the 16 borosilicate-glass absorber tubes was 16 L. Solar–UV irradiation was measured by two radiometers (Ecosystem, model ACADUS-85), which allowed for the measuring of received irradiation as UV-A (300–400 nm) and UV–vis (400–600 nm), respectively. By means of a PLC (programmable logic controller) coupled with the radiometers, they provided data in terms of incident solar power, W m^{-2}, and accumulated solar energy, W h.

2.2.2. Artificial UV-A/C pilot plant

The UV pilot plant (FLUORACADUS-08/2.2) is also shown in Fig. 1 and consisted of a 28-L reactor (2240 mm × 730 mm × 100 mm), with two UV-C lamps (200–280 nm; PHILIPS TUV TL D 55W HO SLV UV-C) and two UV-A lamps (320–400 nm; PHILIPS CLEO Effect 70 W SLV). Both UVC (for photolysis of H_2O_2) and UVA (for ferrioxalate-complex photochemical reactions) were used at the same time. This reactor is constructed in borosilicate 7 mm thick and protected externally by a polypropylene tube. It accommodates four quartz tubes of 34 mm diameter y 1.5 mm thick, where lamps are housed. Temperature (up to 60 °C) was controlled by a digital Fuji PXR4TAY1-1 V controller. For every reaction, a reservoir was

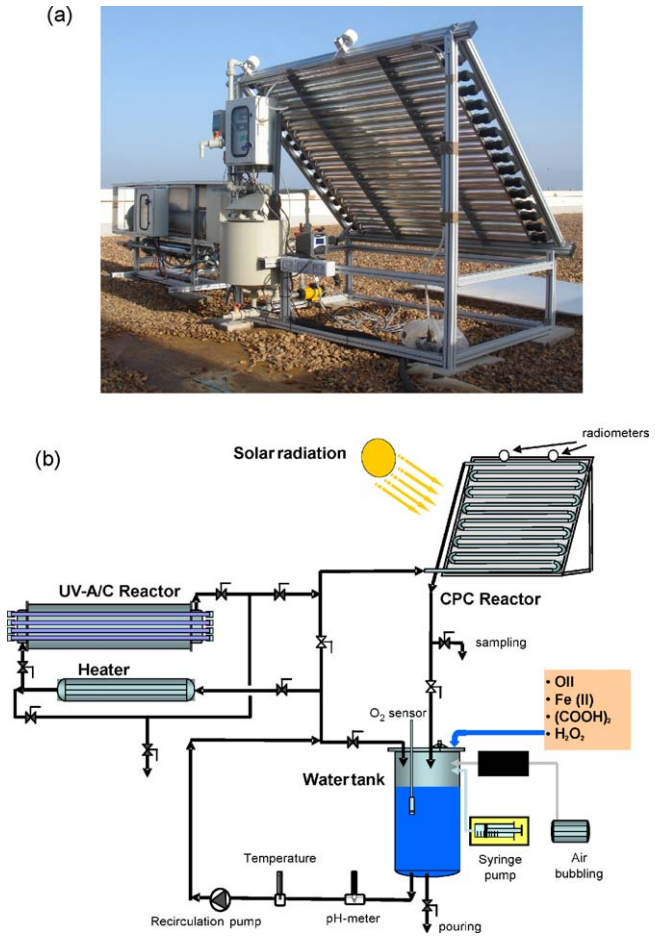

Fig. 1. Experimental set-up based on a CPC and artificial UV-A/C pilot plants; (a) photo; (b) schematic.

charged with 50 L of dye solution and chemicals, and it was continuously pumped (flow rate: 30 L min^{-1}) into the UV-A/C reactor and afterwards into the CPC reactor. After flowing through all the tubes, solution was again recirculated back to the reservoir.

2.3. Analysis

Changes in the Orange II concentration were determined from the absorbance at 486 nm (its maximum absorption wavelength) using a UV–vis Spectrophotometer (Zuzi 4418PC). Interference by intermediate oxidation products did not occur. The degree of mineralization was followed by TOC variation determined with a TOC-5050 Shimazdu analyzer (standard deviation <0.2 mg L^{-1}). The TOC contribution of the added oxalic acid had a relatively low significance as ferrioxalate is easily photolyzed, leading to the mineralization of oxalate. H_2O_2 in solution was determined by titration through an aqueous solution of potassium permanganate (0.02 M) using an automatic Titrino SET/MET 702 (Metrohm).

Table 1
The 5-factor central-composite design matrix and the values of the response functions, k_d and k_{TOC}. Ferrioxalate-assisted combined (UV-A/C–solar) photo-Fenton system with continuous addition of hydrogen peroxide. Initial concentration of dye = 20 ppm; hydrogen peroxide initial concentration: 75 ppm.

Experiments	H_2O_2 flow (mL min^{-1})	[Fe(II)] (ppm)	UV-A/C Time (min)	[$H_2C_2O_4$] (ppm)	pH	k_d (W^{-1} h^{-1})	k_{TOC} (W^{-1} h^{-1})	T^* (°C)	Solar power* ($W m^{-2}$)
1	0.71	7.10	35.51	42.61	4.84	0.169	0.081	21.0	39.9
2	0.29	7.10	35.51	42.61	4.84	0.630	0.091	22.4	14.5
3	0.71	2.90	35.51	42.61	4.84	0.194	0.031	24.4	37.8
4	0.29	2.90	35.51	42.61	4.84	0.268	0.059	30.4	21.9
5	0.71	7.10	14.49	42.61	4.84	0.349	0.039	28.1	36.4
6	0.29	7.10	14.49	42.61	4.84	0.184	0.029	25.9	35.3
7	0.71	2.90	14.49	42.61	4.84	0.106	0.015	27.5	46.7
8	0.29	2.90	14.49	42.61	4.84	0.073	0.010	25.0	43.1
9	0.71	7.10	35.51	17.39	4.84	0.121	0.031	25.3	52.0
10	0.29	7.10	35.51	17.39	4.84	0.212	0.078	26.0	27.9
11	0.71	2.90	35.51	17.39	4.84	0.032	0.005	23.5	36.8
12	0.29	2.90	35.51	17.39	4.84	0.110	0.017	23.6	20.6
13	0.71	7.10	14.49	17.39	4.84	0.1342	0.020	27.2	41.8
14	0.29	7.10	14.49	17.39	4.84	0.248	0.029	26.7	52.4
15	0.71	2.90	14.49	17.39	4.84	0.157	0.012	27.7	47.2
16	0.29	2.90	14.49	17.39	4.84	0.174	0.041	27.0	35.0
17	0.71	7.10	35.51	42.61	3.16	0.423	0.077	27.8	47.1
18	0.29	7.10	35.51	42.61	3.16	0.560	0.081	23.6	46.3
19	0.71	2.90	35.51	42.61	3.16	0.198	0.060	26.2	37.1
20	0.29	2.90	35.51	42.61	3.16	0.174	0.053	27.3	67.0
21	0.71	7.10	14.49	42.61	3.16	0.315	0.129	26.5	44.6
22	0.29	7.10	14.49	42.61	3.16	0.634	0.077	27.3	38.8
23	0.71	2.90	14.49	42.61	3.16	0.277	0.046	24.5	37.1
24	0.29	2.90	14.49	42.61	3.16	0.333	0.058	27.4	38.6
25	0.71	7.10	35.51	17.39	3.16	0.469	0.077	24.2	38.0
26	0.29	7.10	35.51	17.39	3.16	0.177	0.043	27.0	58.0
27	0.71	2.90	35.51	17.39	3.16	0.282	0.047	27.6	51.0
28	0.29	2.90	35.51	17.39	3.16	0.190	0.036	25.1	57.4
29	0.71	7.10	14.49	17.39	3.16	0.733	0.083	27.3	37.4
30	0.29	7.10	14.49	17.39	3.16	0.377	0.071	27.1	45.7
31	0.71	2.90	14.49	17.39	3.16	0.2625	0.037	28.1	43.0
32	0.29	2.90	14.49	17.39	3.16	0.352	0.053	27.6	29.1
33	1.00	5.00	25.00	30.00	4.00	0.762	0.143	30.5	27.8
34	0.00	5.00	25.00	30.00	4.00	0.506	0.072	28.8	42.7
35	0.50	10.00	25.00	30.00	4.00	0.737	0.146	27.9	42.6
36	0.50	0.00	25.00	30.00	4.00	0.094	0.023	29.0	46.5
37	0.50	5.00	50.00	30.00	4.00	0.437	0.083	28.2	31.2
38	0.50	5.00	0.00	30.00	4.00	0.116	0.029	29.5	33.3
39	0.50	5.00	25.00	60.00	4.00	0.147	0.037	28.5	44.1
40	0.50	5.00	25.00	0.00	4.00	0.153	0.019	30.2	46.4
41	0.50	5.00	25.00	30.00	6.00	0.081	0.010	29.6	31.0
42	0.50	5.00	25.00	30.00	2.00	0.269	0.049	30.6	25.3
43	0.50	5.00	25.00	30.00	4.00	0.601	0.075	28.7	26.1
44	0.50	5.00	25.00	30.00	4.00	0.586	0.072	28.1	25.0
45	0.50	5.00	25.00	30.00	4.00	0.593	0.072	27.2	21.2
46	0.50	5.00	25.00	30.00	4.00	0.596	0.078	28.0	26.3
Codified levels									
(+α)	1.00	10.00	50.00	60.00	6.00				
(−α)	0.00	0.00	0.00	0.00	2.00				
(+1)	0.71	7.10	35.51	42.61	4.84				
(−1)	0.29	2.90	14.49	17.39	3.16				
(0)	0.50	5.00	25.00	30.00	4.00				
Additional experiments									
47[a]	0.00	0.00	25.00	0.00	4.00	0.002	0.004	31.7	42.1
48[b]	0.50	5.00	25.00	30.00	4.00	0.507	0.184	33.6	39.9
49[c]	0.50	5.00	25.00	30.00	4.00	0.508	0.188	34.33	28.4

[a] Single UV-A/C/solar treatment, only dye without chemicals.
[b] UV-A/solar treatment.
[c] UV-C/solar treatment.
* Average temperature (T) and incident solar power.

2.4. Experimental design

A central-composite experimental design was applied to investigate the effects of five variables (H_2O_2 flow rate, pH, UV-A/C-lamp exposure time (UVL), and initial concentrations of Fe(II) and oxalic acid) in the ferrioxalate-assisted combined (UV-A/C–solar) photo-Fenton process with continuous addition of H_2O_2 (Table 1). Here, the initial concentration of dye was a constant and thus not considered as a factor. It is well known that the increase of initial dye concentration decreases degradation efficiency because the path length of a photon entering the solution, and thus the amount of hydroxyl radicals generated, is decreased, so the probability of reaction is also decreased.

The design consisted of three series of experiments [14]:

(i) a 2^k factorial design (all possible combinations of the codified values +1 and −1) which in the case of $k = 5$ variables consisted of 32 experiments (Experiments 1–32),
(ii) axial or star points (codified values $\alpha = 2^{k/4} = \pm 2.378$) consisting of $2^k = 10$ experiments (Experiments 33–42),
(iii) replicates of the central point (four experiments, 43–46).

Three additional experiments (47–49) were carried out to complete the degradation study. Temperature and incident solar power were not controlled during the experiment, but they were measured during the reactions, so that their average values were included in the fitting. It was found that both the initial rates of decolorization and mineralization of Orange II solutions obeyed pseudo-first-order kinetics, in agreement with previous works [12,13]. The values of k_d (the decolorization-rate pseudo-constant, $W^{-1}\,h^{-1}$) and k_{TOC} (the mineralization-rate pseudo-constant, $W^{-1}\,h^{-1}$) were related to the accumulated solar energy received by the water solution.

2.5. Neural network strategy

In this work, a linear basis function (a linear combination of inputs, X_j, and weight factors, W_{ij}) was used. Each neural network was solved with two neurons and used a simple exponential activation function [15,16]. The strategy was based on a back-propagation calculation. Parameters were found using the solver tool in Excel using the Marquardt non-linear fitting algorithm [17]. Further details can be found in the literature [18]. Finally, a measure of the saliency of the input variables was made based upon the connection weights of the NNs. This allowed for analysis of the relevance of each variable with respect to the others (expressed as a percentage).

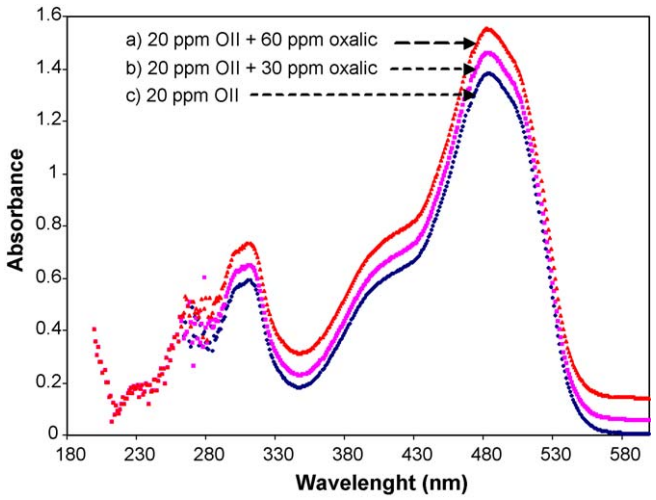

Fig. 2. Effect of oxalic-acid concentration on absorption spectrum of OII solutions.

3. Results and discussion

3.1. Previous studies

Table 2 shows a comparative study on the degradation of Orange II solutions under different systems; both decolorization and mineralization of dye solutions due to direct photolysis using single or combined solar and artificial UV-A/C light were almost negligible. The use of combined solar and artificial UV light sources in the presence of only the Fe(II) catalyst also gave insignificant color removal (10.9%) and TOC removal (4.3%) due to the fact that hydroxyl radicals are not generated by ferrous ions in the absence of H_2O_2. If the irradiation of dye solution under combined-light sources was carried out adding only oxalic acid, color removal increased up to 52% as contaminant–oxalate complexes are formed that absorb more radiation from the solar spectrum and thus break down the chromophore group of the molecule responsible for the color of the azo dye. This effect is evident in Fig. 2, showing the three absorption spectra of single OII solutions and of the dye plus 30 or 60 ppm of oxalic acid. However, hydroxyl radicals were not generated, and TOC removal was still lower than 6%. All the other systems studied used an electron acceptor such as hydrogen peroxide, and they all led to 100% decolorization, although with different reaction rates depending on operating conditions. Orange II degradation due to H_2O_2 alone in the dark was also very slow, as previously reported by the authors [12]. TOC removal efficiency under the solar/UV-A/C/H_2O_2 system was low but still higher (14.2%) than that obtained under single-solar, UV-A/C or solar/UV-

Table 2
Orange II solutions degradation. A comparative study.

System	k_d ($W^{-1}\,h^{-1}$)	Color removal (%)	k_{TOC} ($W^{-1}\,h^{-1}$)	TOC removal (%)
Solar	0.001	11.0	0.0004	4.0
UV-A/C	0.001	18.0	0.0043	3.6
Solar/UV-A/C	0.002	21.6	0.0047	14.8
Solar/H_2O_2/Fe/oxalic (addition of H_2O_2 at the beginning of reaction)[a]	0.491	100	0.0637	80.0
Solar/H_2O_2/Fe/oxalic (continuous addition of H_2O_2)[b]	0.475	100	0.1820	95.0
Solar/UV-A/C/H_2O_2	0.019	100	0.0004	4.2
Solar/UV-A/C/Fe	0.001	10.9	0.0004	4.3
Solar/UV-A/C/oxalic	0.012	52.0	0.0047	5.9
Solar/UV-A/C/H_2O_2/Fe/oxalic	0.762	100	0.1983	99.0
Solar/UV-A/H_2O_2/Fe/oxalic	0.507	100	0.1840	96.0
Solar/UV-C/H_2O_2/Fe/oxalic	0.508	100	0.1880	97.0

[a] Reference [12].
[b] Reference [13].

A/C systems (~4%), which indicates the favorable synergistic effect of hydrogen peroxide and UV-C light. This can possibly be due to the fact that, although •OH radicals are generated from the direct photolysis of H_2O_2 under artificial UV-C light, their concentration is not sufficient to mineralize dye solutions. Regarding the ferrioxalate-assisted solar photo-Fenton processes, the mineralization efficiency increased to 95% with continuous H_2O_2 dosing during the reaction, as previously reported [13], but that process presents a drawback because the reaction times in solar installations on cloudy days are long. The values of k_d and k_{TOC}, calculated as a function of accumulated solar energy, were similar on both cloudy and sunny days, but the reaction times were longer on cloudy days because the solar power was lower. To overcome this disadvantage, a combined system of UV-A/C-lamp exposure in series with a solar-CPC pilot plant could solve this problem. Additionally, the degradation efficiency could be increased due to the continuous regeneration of Fe^{2+} via photoreduction of Fe^{3+} with 200–400 nm UV light and extra generation of new •OH radicals with H_2O_2. In our previous study, we noted that the solar/UV-A/C–H_2O_2/Fe/oxalic-acid process was the most efficient system for both decolorization and mineralization of dye solutions, reaching 100% color removal in 15 min and 99% TOC removal in 45 min (50 W h) with higher rate constants (k_d = 0.762 W^{-1} h^{-1}; k_{TOC} = 0.1983 W^{-1} h^{-1}). The use of UV-A (320–400 nm) lamps or UV-C (200–280 nm) lamps alone coupled with solar light did not affect the percentage color removal (100% in both cases) or k_d, but the mineralization degree (97%; time = 50 min) and k_{TOC} (0.1880 W^{-1} h^{-1}) were higher under UV-C irradiation than with UV-A light because the decomposition of H_2O_2 to form hydroxyl radicals mainly uses photons below 300 nm. On the other hand, in the system with UV-A, TOC removal (96% in 54 min) was higher than that of the solar/H_2O_2/Fe/oxalic process (95% in 59 min) as 320–400 nm irradiation favors the ferrioxalate photochemistry. Taking into account these results from the previous study, a central-composite experimental design was applied to optimize the solar/UV-A/C–H_2O_2/Fe(II)/oxalic-acid process, since this solar/UV-activated catalytic system can offer an economical and practical alternative for the destruction of this type of contaminant.

3.2. Combined artificial UV-A/C and solar pilot plants

All the experiments presented in this section are based on the degradation of dye solutions in a ferrioxalate-assisted photo-Fenton system with continuous addition of hydrogen peroxide irradiated under combined artificial UV-A/C and solar light. In all of them, the disappearance of Orange II and TOC removal followed pseudo-first-order kinetics with respect to the dye and total organic carbon concentrations, respectively. In order to study the effect of the variables hydrogen peroxide flow rate, pH, UV-lamp exposure time (UVL) and initial concentrations of Fe(II) and oxalic acid on the response functions, i.e., decolorization (k_d) and mineralization (k_{TOC}) rate constants, a central-composite design was performed. The complete experimental design matrix, variable ranges and results for k_d and k_{TOC} are shown in Table 1. Temperature and solar power were not controlled during the experiment, but they were measured during the reaction, so their average values were included in the fitting.

Experimental results and NN predictions of these constants were in good agreement, with an average error lower than 13% and 11% for decolorization and mineralization, respectively. The equation and fitting parameters for k_d and k_{TOC} are shown in Table 3. N_1 and N_2 are general factors related to the first and the second neuron, respectively. W_{11} to W_{17} are the contribution parameters to the first neuron and represent the influence of each

Table 3
Equation and parameters of neural network fittings for Orange II solutions decolorization and mineralization under the process Ferrioxalate-assisted combined UV-A/C–solar photo-Fenton with continuous addition of hydrogen peroxide.

Neural network fitting			
Equation[a]	Decolorization/mineralization		
	k_d/k_{TOC} [W^{-1} h^{-1}] = $N_1 \times (1/(1+1/EXP([H_2O_2\ flow] \times W_{11} + [Fe] \times W_{12} + [pH] \times W_{13} + [H_2C_2O_4] \times W_{14} + [Temperature] \times W_{15} + [Solar\ Power] \times W_{16} + [UVL] \times W_{17})))$ + $N_2 \times (1/(1+1/EXP([H_2O_2\ flow] \times W_{21} + [Fe] \times W_{22} + [pH] \times W_{23} + [H_2C_2O_4] \times W_{24} + [Temperature] \times W_{25} + [Solar\ Power] \times W_{26} + [UVL] \times W_{27})))$		
Weight factors	Parameter	Values of neurons and factors to obtain the decolorization kinetic rate constant of dye solutions, k_d	Values of neurons and factors to obtain the mineralization kinetic rate constant of dye solutions, k_{TOC}
N_1	Neuron	−2.1666	−0.5449
W_{11}	H_2O_2 flow	−0.7641	−3.4719
W_{12}	[Fe(II)]	0.4469	1.3002
W_{13}	pH	−13.4483	−9.2126
W_{14}	$[H_2C_2O_4]$	10.6664	3.4212
W_{15}	Temperature	−0.2319	0.9849
W_{16}	Solar power	2.1618	0.0837
W_{17}	UVL	5.0320	4.0397
N_2	Neuron	2.4671	0.6065
W_{21}	H_2O_2 flow	−0.9687	−3.1945
W_{22}	[Fe(II)]	1.9177	2.0245
W_{23}	pH	−13.5217	−8.8464
W_{24}	$[H_2C_2O_4]$	4.4696	3.2416
W_{25}	Temperature	1.3354	1.1143
W_{26}	Solar power	0.9306	−0.2100
W_{27}	UVL	4.7468	3.8077

Saliency analysis of the input variables for the neural network (%)							
Neural network output	Parameters						
	H_2O_2 flow	[Fe]	pH	$[H_2C_2O_4]$	Temperature	Solar power	UVL
Decolorization kinetic rate constant, k_d (W^{-1} h^{-1})	4.69	5.17	24.24	24.63	3.29	10.03	27.96
Mineralization kinetic rate constant, k_{TOC} (W^{-1} h^{-1})	20.17	9.40	19.71	20.08	6.19	0.78	23.67

[a] Parameters values in equations must be previously normalized to the (0.1) interval.

of the seven variables in the process (H_2O_2 flow rate, [Fe(II)], pH, [$H_2C_2O_4$], average temperature, average incident solar power and UVL); W_{21}–W_{27} are the contributions to the second neuron corresponding to the same variables.

The results of a saliency analysis on the input variables for each neural network are also shown in Table 3. From these results, it was possible to deduce the effect of each parameter on the studied variables, reported as percentages. It was confirmed that, over the studied range, UV-lamp exposure time was the most significant factor affecting both the decolorization and mineralization kinetics. The pH and oxalic-acid concentration also had significant influences on both constants, the H_2O_2 flow rate had a higher effect on mineralization, and the effect of Fe concentration on mineralization was twice that its effect on decolorization, as explained below.

3.2.1. Effect of pH and H_2O_2 flow rate

Fig. 3 shows a simulation analysis example from the NNs (the equation shown in Table 3). The effect of the variables hydrogen peroxide flow rate and pH on the value of the decolorization rate constant, k_d, can be seen (operating conditions: average temperature, 30 °C; [Fe(II)], 2 mg L^{-1}; [$(COOH)_2$], 30 mg L^{-1}; average solar power, 25.3 W m^{-2}; and UVL, 25 min). Decolorization of the dye solutions was favored at pH values between 2 and 4; in this interval, the k_d value was at its maximum, and the effect of H_2O_2 flow rate was insignificant over the studied range. It is possible that this is because all added hydrogen peroxide is consumed immediately and controls the reaction rate. Thus, two balanced, opposing effects occur: the concentration of hydrogen peroxide in solution is increased when hydrogen peroxide flow rate is increased and by generation during the photo-oxidation process in the presence of ferrioxalate [3] according to Eqs. (1)–(6) as a function of Fe and oxalic-acid concentrations. Conversely, hydrogen peroxide is consumed by reaction with Fe(II) to form •OH radicals by Eq. (1), by self-decomposition to form H_2O and O_2 according to Eq. (8), by direct photolysis (Eq. (9)), by reaction with •OH radicals (Eq. (7)) and by direct/molecular oxidation reaction with dye molecules. As reported previously [13], in this optimal pH range, more •OH radicals are produced by the reaction of ferrous ions (generated by photolysis of $[Fe(C_2O_4)_2]^-$ and $[Fe(C_2O_4)_3]^{-3}$ under solar–UV light) with hydrogen peroxide according to Eq. (1).

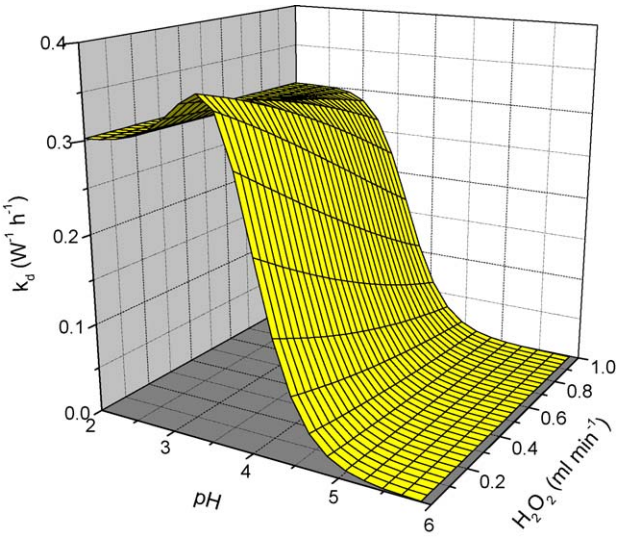

Fig. 3. NN simulation of the effect of pH and H_2O_2 flow rate on the Orange II decolorization constant, k_d. [Orange II] = 20 mg L^{-1}; [Fe(II)] = 2 mg L^{-1}; [$H_2C_2O_4$] = 30 mg L^{-1}; UVL, 25 min; accumulated solar energy, 50 W h; average temperature, 30 °C; an average solar power, 25.3 W m^{-2}.

Above this optimum pH, the process efficiency decreases because Fe(III)-complex coagulation reduces the catalyst effect of Fe(II) for decomposing H_2O_2. The increase of hydrogen peroxide dosage has a negative effect on decolorization because an excess of hydrogen peroxide reduces catalytic activity, as it favors reactions (1) and (7), diminishing the amount of H_2O_2 and •OH radicals available to destroy Orange II. Although other radicals are generated ($HO_2^•$), their oxidation potential is much smaller than that of the hydroxyl radicals.

$$H_2O_2 + Fe^{2+} \rightarrow Fe^{3+} + {}^•OH + OH^- \quad (1)$$

$$[Fe(C_2O_4)_3]^{3-} + h\nu \rightarrow Fe^{2+} + 2\,C_2O_4{}^{2-} + C_2O_4{}^{•-} \quad (2)$$

$$C_2O_4{}^{•-} + [Fe(C_2O_4)_3]^{3-} \rightarrow Fe^{2+} + 3C_2O_4{}^{2-} + 2CO_2 \quad (3)$$

$$C_2O^•{}_4{}^- + O_2 \rightarrow O_2{}^{•-} + 2CO_2 \quad (4)$$

$$O^•{}_2{}^- + H + \rightarrow HO_2^• \quad (5)$$

$$HO_2^• + HO_2^• \rightarrow H_2O_2 + O_2 \quad (6)$$

$$H_2O_2 + {}^•OH \rightarrow HO_2^• + H_2O \quad (7)$$

$$2H_2O_2 \rightarrow O_2 + 2H_2O \quad (8)$$

$$H_2O_2 + h\nu \rightarrow 2{}^•OH \quad (9)$$

When the pH value increases from 5 to 6, the Fe^{3+} and Fe^{2+} species are almost nonexistent in solution, and the predominant species of Fe is $Fe(OH)_3$ as a precipitate, which is barely photoactive and cannot be regenerated to the ferrous ion, as noted by previous authors [19].

Regarding the mineralization of Orange II solutions, as shown in Fig. 4, optimal pH and continuous addition of H_2O_2 to the system could either increase the reaction rate or cause inhibition effects depending on operating conditions. Thus, when the reaction was conducted using only the initial amount of 75 mg L^{-1} 1 H_2O_2, without further continuous addition of hydrogen peroxide the increase of pH increased the self-decomposition rate of hydrogen peroxide, as is well known, and thus decreased the mineralization rate when an initial concentration of 2 mg L^{-1} Fe(II) was used since there was an insufficient amount of ferrous iron remaining to decompose the hydrogen peroxide present and hydroxyl radicals were not generated. When the initial concentration of Fe(II) was increased to 10 mg L^{-1}, an optimal pH value was reached near pH 4. It can be seen that pH positively affected the mineralization rate up to an optimal pH value, but only when the initial ferrous concentration used was greater than 5 mg L^{-1}, and this optimal pH value diminished as the H_2O_2 flow rate was increased. Above the optimal ratio of pH to H_2O_2 flow rate, the increase of H_2O_2 flow rate decreased k_{TOC} values as an inhibition effect due to •OH scavenging was caused by excess hydrogen peroxide (Eq. (7)).

3.2.2. Effect of UVL and initial concentration of oxalic acid

Fig. 5a and b shows (as an example) the effect of the variables UVL and initial concentration of oxalic acid on k_d and k_{TOC}, respectively, as simulated by NNs (operating conditions: H_2O_2 flow rate, 0.5 mL min^{-1}; pH, 3.5; average temperature, 27 °C; average solar power, 35 W m^{-2}; and Fe(II), 2 mg L^{-1}).

As shown in Fig. 5a, over the studied range oxalic-acid addition positively affected the decolorization of Orange II solutions in the ferrioxalate-assisted combined solar/UV–photo-Fenton system until an optimal concentration was reached, which depended on the UV-A/C-lamp exposure time (total decolorization was reached

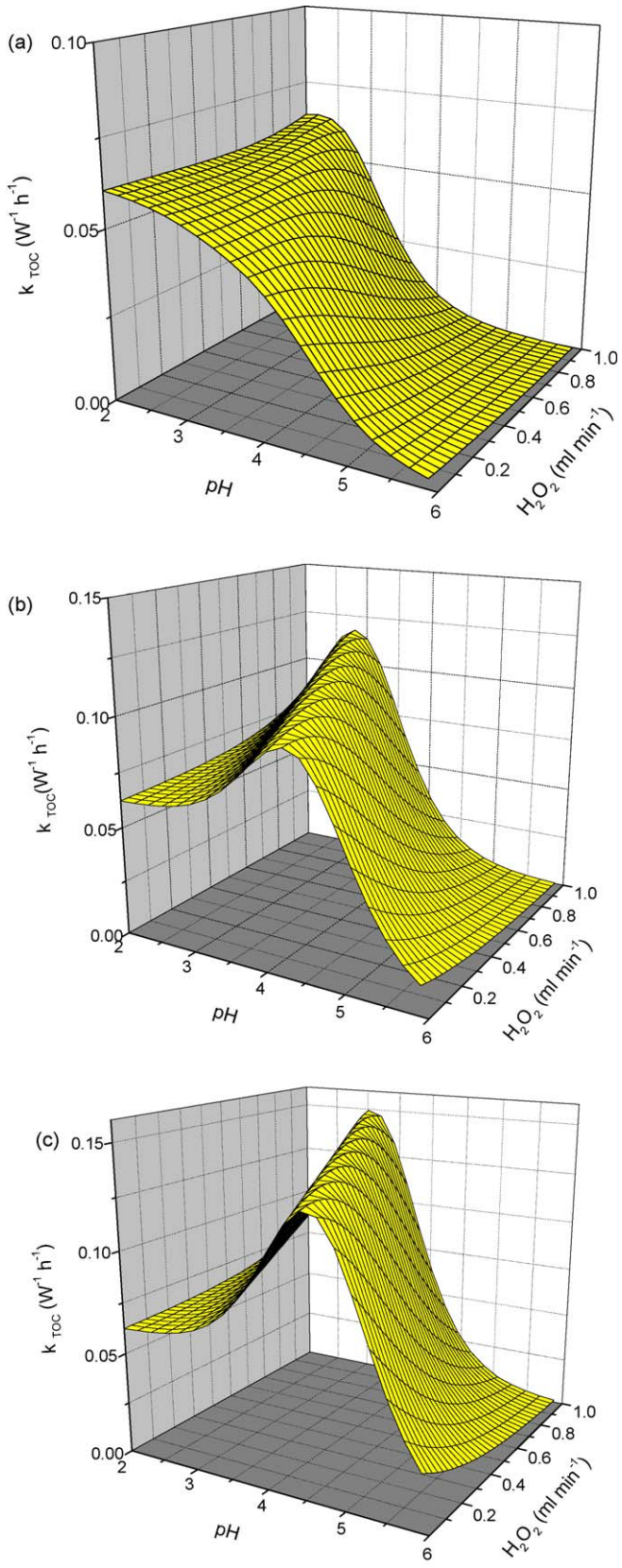

Fig. 4. NN simulation of the effect of pH and H_2O_2 flow rate on Orange II mineralization constant, k_{TOC}; [Orange II] = 20 mg L^{-1}; UVL, 25 min; average temperature, 27 °C; solar power, 35 W m^{-2}; accumulated solar energy, 50 W h; [($H_2C_2O_4$)] = 30 mg L^{-1}. (a) [Fe(II)] = 2 mg L^{-1}; (b) [Fe(II)] = 7 mg L^{-1}; (c) [Fe(II)] = 10 mg L^{-1}.

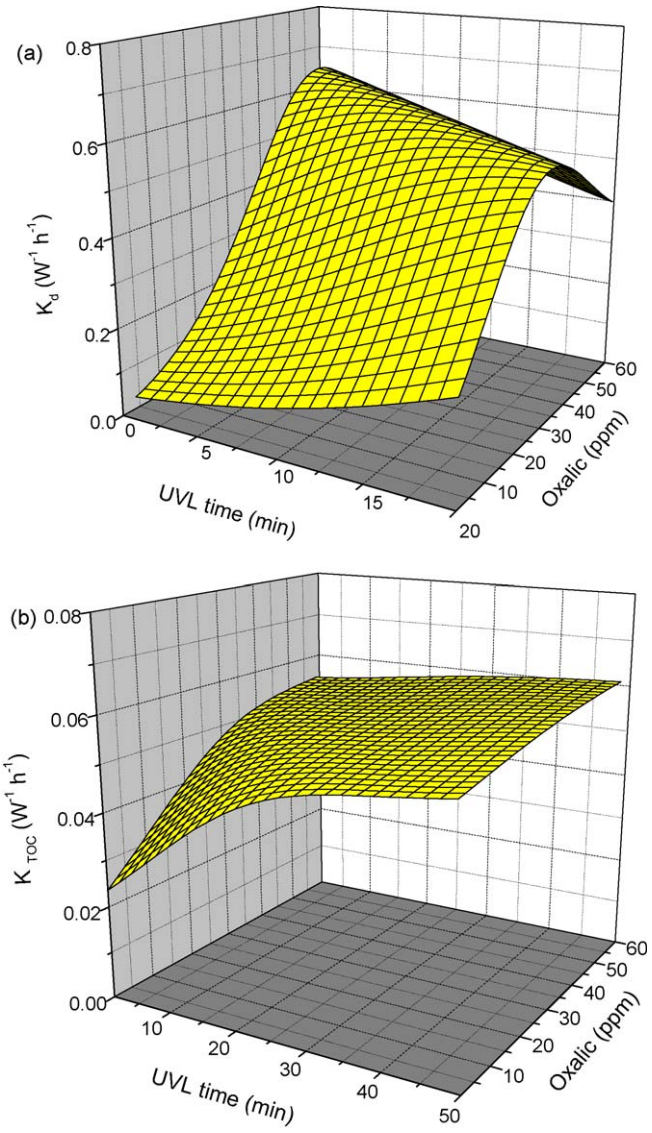

Fig. 5. NN simulation of the effect of UVL and initial concentration of oxalic acid on Orange II decolorization; (a) mineralization constants; (b) H_2O_2 flow rate, 0.5 mL min^{-1}; pH, 3.5; average temperature, 27 °C; average solar power, 35 W m^{-2}; accumulated solar energy, 50 W h; [Fe(II)]: 2 mg L^{-1}.

in 20 min). This optimal initial oxalic-acid concentration value diminished as the UVL increased due to the faster generation of Fe^{2+} ion by photolysis of ferrioxalate and the additional hydroxyl radicals produced by Eqs. (1)–(6). The photolysis of ferrioxalate also generates extra H_2O_2 and is thus a continuous source of Fenton's reagent. However, when higher UVL and oxalic values were used, the decolorization efficiency decreased, possibly due to the fact that the excess of generated hydrogen peroxide may scavenge the hydroxyl radicals according to Eq. (7), decreasing the amount of hydrogen peroxide in solution. Taking into account the effect of these parameters on Orange II mineralization (Fig. 5b), it can be concluded that the direct or molecular reaction of H_2O_2 with OII molecules plays an important role in decolorization. Fig. 5b shows that over the studied range of these two variables, both parameters positively affected k_{TOC}, although the amount of hydrogen peroxide decreases it above a certain point, as mentioned above. The effect of oxalic-acid addition was more significant for lower UV-lamp exposure times as less excess H_2O_2 was generated, so more hydroxyl radicals were available to attack the intermediate compounds, indicative of the main role of the radical reaction

on mineralization; further confirmation of this will also be discussed in Section 3.3.

Two degradation trials of Orange II solutions were also carried out under the same conditions shown in Fig. 5b, but here combining solar light with artificial UV-A or UV-C light irradiation (Table 2). These trials resulted in 100% color removal in both cases, which indicates that in a solar/UV-A system (recall that above 300 nm photolysis of H_2O_2 does not take place), decolorization is mainly by molecular or direct reaction of the OII molecule with hydrogen peroxide. However, TOC removal was higher when sunlight and UV-C (200–300 nm) or UV-A (320–400 nm) irradiation were combined because more hydroxyl radicals were primarily generated by photolysis of hydrogen peroxide (97% TOC removal) or by ferrioxalate photochemistry (96% TOC removal), and the reactions were faster than the solar-only process, confirming the main role of free radicals.

3.3. Degradation on cloudy days

The degradation of Orange II solutions was again carried out under the same conditions shown in Fig. 5b, but this time with only artificial UV-A/C light irradiation, as the solar power was below 10 W m^{-2} (a typical cloudy day). The results obtained were 100% decolorization in 10 min and 96% TOC removal in 52 min, which indicates that the use of UV-A/C lamps can be used as an alternative to solar CPC when atmospheric conditions are unfavorable.

3.4. Kinetics and degradation mechanism study

Additional experiments were carried out to evaluate the possible degradation mechanisms. The results, shown in Table 4, revealed that the Orange II-degradation process in the ferrioxalate-assisted combined solar/UV-A/C–photo-Fenton system can be described by a mechanism involving decolorization by a direct-oxidation reaction with H_2O_2, degradation by photolytic breakdown of dye–oxalate complex chromophore groups and decolorization and mineralization by radical reaction (mainly with $^{\bullet}OH$). A radical mechanism implies non-selective radical reactions with dye molecules and intermediates to form CO_2, H_2O and inorganic species, thus diminishing the TOC values, as previously reported [13].

The objective of this section was to determine the contribution of each of these mechanisms to the overall decolorization or/and mineralization reactions. Thus, it was assumed that the reaction mechanism for the Orange II degradation (decolorization/mineralization) was split into three individual steps:

(1) Direct or molecular reaction with H_2O_2:

$$\mathrm{OII} + \mathrm{H_2O_2} \rightarrow \mathrm{products} - r_D = \left(-\frac{dC_{\mathrm{OII/TOC}}}{di}\right)_D = k_D C_{\mathrm{OII/TOC}} C_{\mathrm{H_2O_2}} \quad (10)$$

(2) Photolytic breakdown in the chromophore group of dye–oxalate complexes:

$$\mathrm{OII\text{-}oxalate} + h\nu \rightarrow \mathrm{products} - r_{\mathrm{Ph}} = \left(-\frac{dC_{\mathrm{OII/TOC}}}{di}\right)_{\mathrm{Ph}} = k_{\mathrm{Ph}} C_{\mathrm{OII/TOC}} C_{\mathrm{Ph}} \quad (11)$$

(3) Oxidation of Orange II by free radicals (mainly $^{\bullet}OH$):

$$\mathrm{OII} + {}^{\bullet}\mathrm{OH} \rightarrow \mathrm{products} - r_R = -\left(\frac{dC_{\mathrm{OII/TOC}}}{di}\right)_R = k_R C_{\mathrm{OII/TOC}} C_{{}^{\bullet}\mathrm{OH}} \quad (12)$$

Then, the overall rate of Orange II degradation can be expressed as a sum of the contributions of Eqs. (10)–(12) as follows:

$$-\left(\frac{dC_{\mathrm{OII/TOC}}}{di}\right)_{\mathrm{overall}} = r_D + r_{\mathrm{Ph}} + r_R = k_D C_{\mathrm{OII/TOC}} C_{\mathrm{H_2O_2}} + k_{\mathrm{Ph}} C_{\mathrm{OII/TOC}} C_{\mathrm{Ph}} + k_R C_{\mathrm{OII/TOC}} C_{{}^{\bullet}\mathrm{OH}} \quad (13)$$

where r_D, r_{Ph} and r_R represent the molecular/direct reaction with H_2O_2, photolytic breakdown and radical reaction rates, respectively, k_d, k_{Ph} and k_R are the apparent rate constants for the direct, photolytic and radical reactions, respectively, $C_{\mathrm{OII/TOC}}$, $C_{\mathrm{H_2O_2}}$, C_{Ph} and $C_{{}^{\bullet}\mathrm{OH}}$ are the concentrations of dye/TOC, hydrogen peroxide, photons and hydroxyl radicals, respectively, and i is the accumulated solar energy.

It can be assumed for simplicity that the average H_2O_2, photon and $^{\bullet}OH$ radical concentrations were constant over the reaction time and can therefore be included in the pseudo-first-order kinetics rate constants according to Eq. (14). Thus, the overall decolorization and mineralization rate (Eq. (13)) can be simplified to a pseudo-first-order kinetic law with respect to the dye or TOC

Table 4
Contribution of different reaction mechanisms to overall (decolorization/mineralization) degradation of Orange II solutions.

Ferrioxalate-assisted solar photo-Fenton (calculated from reference [13] data)										
tert-ButOH	Average $C_{H_2O_2}$ (ppm)	k_d	k'_{Dd}	k'_{Phd}	k'_{Rd}	k_{TOC}	k'_{DTOC}	k'_{PhTOC}	k'_{RTOC}	[Fe(II)] ppm
No	110	0.280	0.170	0.006	0.104	0.0450	0	0.0002	0.0448	**5**
Yes	160	0.176	0.170	0.006	0.000	0.0002	0	0.0002	0.0000	**5**
Ferrioxalate-assisted combined solar/UV-A/C photo-Fenton (this work)										
No	0	0.012	0.000	0.006	0.006	0.0047	0	0.0047	0.0000	**0**
Yes	0	0.006	0.000	0.006	0.000	0.0047	0	0.0047	0.0000	**0**
No	115	0.094	0.084	0.006	0.004	0.0230	0	0.0047	0.0183	**0**
Yes	160	0.090	0.084	0.006	0.000	0.0047	0	0.0047	0.0000	**0**
No	80	0.198	0.154	0.006	0.038	0.0610	0	0.0047	0.0563	**2**
Yes	147	0.160	0.154	0.006	0.000	0.0047	0	0.0047	0.0000	**2**
No	65	0.594	0.102	0.006	0.486	0.074	0	0.0047	0.0693	**5**
Yes	135	0.108	0.102	0.006	0.000	0.0047	0	0.0047	0.0000	**5**
No	35	0.737	0.065	0.006	0.666	0.146	0	0.0047	0.1413	**10**
Yes	109	0.071	0.065	0.006	0.000	0.0047	0	0.0047	0.0000	**10**

$[H_2C_2O_4] = 30$ ppm; pH 4; constants in $W^{-1}\,h^{-1}$.

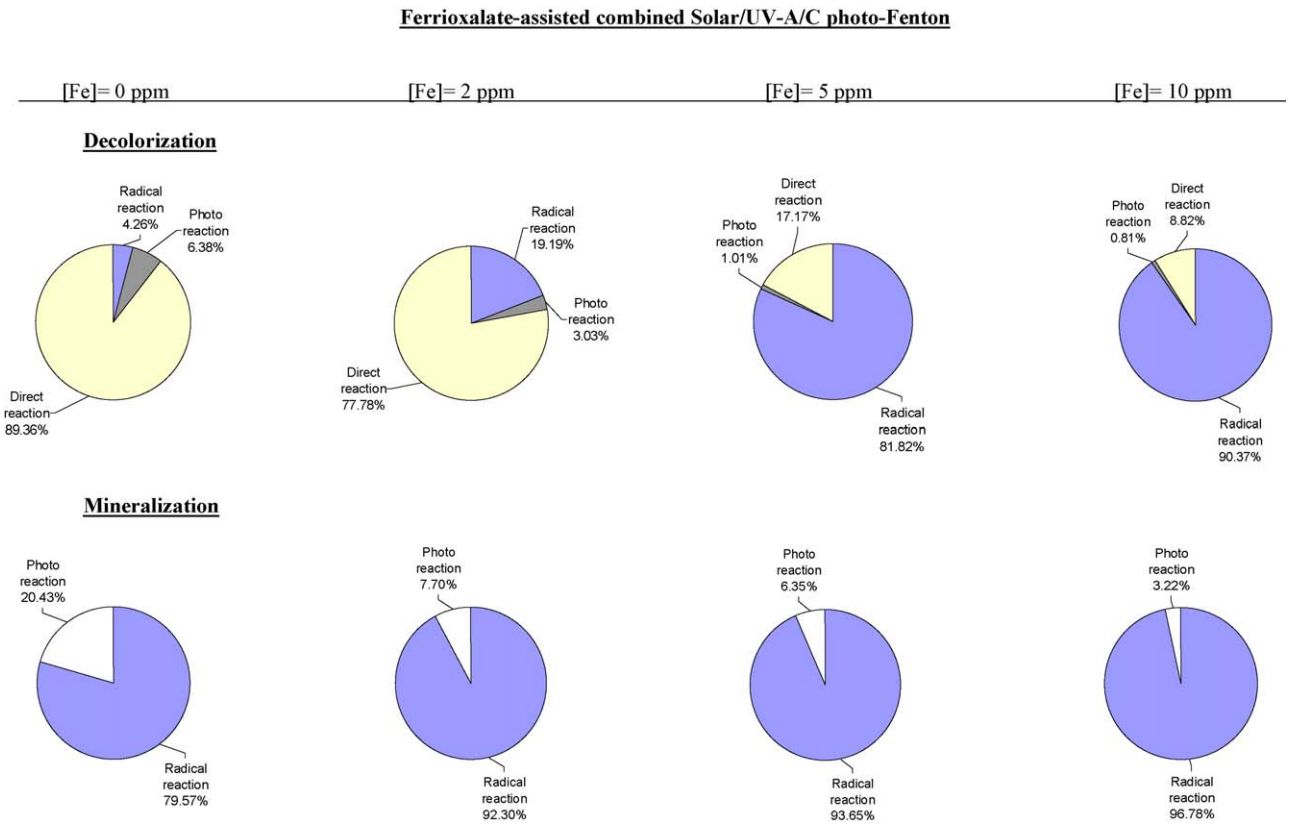

Fig. 6. Contributions of direct, photolytic breakdown and radical reactions to overall decolorization and mineralization reactions.

concentration as follows:

$$\left(-\frac{dC_{\mathrm{OII/TOC}}}{di}\right)_{\mathrm{overall}} = r_D + r_{\mathrm{Ph}} + r_R = k'_D C_{\mathrm{OII/TOC}} + k'_{\mathrm{Ph}} C_{\mathrm{OII/TOC}} + k'_R C_{\mathrm{OII/TOC}} \quad (14)$$

where k'_D, k'_{Ph} and k'_R are the pseudo-first-order kinetics rate constants for the direct/molecular, photolytic and radical reactions, respectively:

$$k'_D = k_D C_{\mathrm{H_2O_2}} \quad (15)$$

$$k'_{\mathrm{Ph}} = k_{\mathrm{Ph}} C_{\mathrm{Ph}} \quad (16)$$

$$k'_R = k_R C_{\bullet\mathrm{OH}} \quad (17)$$

In all the experiments, the disappearance of Orange II and the TOC removal followed pseudo-first-order kinetics with respect to the dye and total organic carbon concentrations, respectively, as follows:

$$r = -\frac{dC_{\mathrm{OII/TOC}}}{di} = kC_{\mathrm{OII/TOC}} \quad (18)$$

where r is the reaction rate, $C_{\mathrm{OII/TOC}}$ is the concentration (mg L^{-1}) of Orange II or TOC at an accumulated solar energy i (W h) and $k = (k'_D + k'_{\mathrm{Ph}} + k'_R)$ is the pseudo-first-order decolorization (k_d) or mineralization (k_{TOC}) rate constant ($W^{-1}\,h^{-1}$) for the degradation reaction. This equation can be integrated between $i = 0$ and $i = i$, yielding:

$$\ln\frac{(C_{\mathrm{OII/TOC}})_{\mathrm{o}}}{C_{\mathrm{OII/TOC}}} = ki \quad (19)$$

where $(C_{\mathrm{OII/TOC}})_{\mathrm{o}}$ is the initial concentration of Orange II or TOC. According to this expression, a plot of the first term vs. i must yield a straight line satisfying Eq. (19) with slope k_d or k_{TOC}.

The direct-reaction rate constant, k'_D, was obtained from experiments under conditions where free radicals, mainly $^{\bullet}$OH, do not occur ($C_{\bullet\mathrm{OH}} = 0$), as in the presence of the radical-scavenging agent tert-butyl alcohol (0.1 M) or in the absence of oxalic acid and Fe. The k'_{Ph} values were calculated from reactions under conditions where the only chemical used was oxalic acid, so in the absence of H_2O_2 and Fe, $^{\bullet}$OH radicals were not present in solution, and direct-oxidation reactions did not take place.

Table 4 shows the importance of the Fe catalyst in the reaction mechanism because of its main role in the Fenton reactions, and the values for the constants of the direct, photolytic breakdown and radical reactions corresponding to decolorization and mineralization phases. All the experiments were carried out both in the presence and in the absence of tert-butyl alcohol. As can be seen, in the presence of tert-butyl alcohol, the mineralization rate is almost negligible as it was only achieved by photolytic breakdown and not by direct reaction with H_2O_2 or reaction with hydroxyl radicals. The k'_{PhTOC} value was higher when the solution was irradiated under combined solar/UV-A/C light due to the faster generation of Fe^{2+} ion by photolysis of ferrioxalate and the higher decomposition of hydrogen peroxide by its homogeneous reaction with Fe, resulting in a lower average H_2O_2 concentration in solution (see the data for both single-solar and combined-light systems for [Fe] = 5 mg L^{-1}), so more additional hydroxyl radicals were produced by Eqs. (1)–(6). In contrast, when the reaction was carried out without H_2O_2 and Fe(II) under the combined-light system, mineralization was due only to light absorption by dye–oxalate complexes and intermediates as $^{\bullet}$OH radicals were not present in solution.

The average hydrogen peroxide concentration in solution decreased when Fe(II) was increased as it acts as a decomposition catalyst, so radical contributions to both decolorization and

mineralization also increased (see Fig. 6). The radical-mechanism contribution to the decolorization rate increased from 4.26 to 90.37% when Fe concentration increased from 0 to 10 mg L^{-1}, diminishing the importance of direct and photolytic reactions under the same conditions because more •OH radicals were available for oxidation. Fig. 6 shows that mineralization by direct reaction with hydrogen peroxide did not take place, and as indicated above, Fe increased the radical mechanism's contribution to mineralization from 79.57 to 96.78%. To achieve mineralization, more aggressive conditions are apparently required than those needed to cleave the chromophore group. Taking into account the results in Fig. 6 and Table 2, when the radical contribution increased, the overall reaction rates also increased as hydroxyl attack is non-selective and faster than direct oxidation.

4. Conclusions

A central-composite design was performed to optimize the degradation of Orange II solutions in a ferrioxalate-assisted combined (solar/UV-A/C) photo-Fenton process with continuous addition of hydrogen peroxide. The cooperation of H_2O_2, Fe(II) and oxalic acid played an important role in the dye mineralization. The low color removal percentage (50%) in the presence of oxalic acid alone with solar–UV-A/C light resulted from the photolytic breakdown of dye–oxalate complex chromophore groups. All of the treatments involving hydrogen peroxide under light irradiation were effective in removing the color of dye solutions. The addition of Fe^{2+} and oxalic acid also promoted the TOC removal of dye solutions, achieving practically complete mineralization (99% in 45 min) in the system under combined solar/UV-A/C light with continuous addition of H_2O_2 to minimize the •OH-scavenger effect. Irradiation with UV-A light favors the ferrioxalate photochemistry. The concentration of Fe catalyst in the system influenced the performance to a considerable extent as the radical-mechanism contribution to overall degradation increased with iron level. On cloudy days, total decolorization and 95% mineralization could be achieved in this UV/A/C-lamp pilot-plant system in the presence of hydrogen peroxide and oxalic also using a ferrous concentration of only 2 ppm. This process can be considered environmentally friendly as it is composed only of atoms of hydrogen, oxygen and carbon, yielding water, CO_2 and hydroxyl ions as final products.

Acknowledgement

The financial support from the Consejería de Educación y Ciencia of the Junta de Comunidades de Castilla-La Mancha (PCI08-0047-4810) is gratefully acknowledged.

References

[1] M. Rodríguez, S. Malato, C. Pulgarín, S. Contreras, D. Curcó, J. Giménez, S. Esplugas, Solar Energy 79 (2005) 360–368.
[2] R.F.P. Nogueira, M.R.A. Silva, A.G. Trovó, Solar Energy 79 (2005) 384–392.
[3] A. Durán, J.M. Monteagudo, E. Amores, Appl. Catal. B: Environ. 80 (2008) 42–50.
[4] S. Malato, J. Blanco, J. Cáceres, A.R. Fernández-Alba, A. Agüera, A. Rodríguez, Catal. Today 76 (2002) 209–220.
[5] J. Feng, X. Hu, P.L. Yue, H.Y. Zhu, G.Q. Lu, Water Res. 37 (2003) 3776–3784.
[6] S. Malato, J. Blanco, M.I. Maldonado, P. Fernández, D. Alarcón, M. Collares, J. Farinha, J. Correia de Oliveira, Solar Energy 77 (2004) 513–524.
[7] R. Bauer, G. Waldner, H. Fallmann, S. Hager, H. Karé, T. Krutzler, S. Malato, P. Maletzky, Catal. Today 53 (1999) 131–144.
[8] R.F.P. Nogueira, A.G. Trovó, D.F. Mode, Chemosphere 48 (2002) 385–391.
[9] M.S. Lucas, J.A. Peres, Dyes Pigment 74 (2007) 622–629.
[10] A. Safarzadeh-Amiri, J.R. Bolton, S.R. Cater, Water Res. 31 (1997) 787–798.
[11] K. Selvam, M. Muruganandham, M. Swaminathan, Sol. Energy Mater. Sol. Cells 89 (2005) 61–74.
[12] J.M. Monteagudo, A. Durán, C. López-Almodovar, Appl. Catal. B: Environ. 83 (2008) 46–55.
[13] J.M. Monteagudo, A. Durán, I. San Martin, M. Aguirre, Appl. Catal. B: Environ. 89 (2009) 510–518.
[14] G.E.P. Box, W.G. Hunter, J.S. Hunter, Statistics for Experimenters: An Introduction to Design, Data Analysis and Model Building, Wiley, New York, 1978.
[15] D.P. Morgan, C.L. Scofield, Neural Networks and Speech Processing, Kluwver Academic Publishers, London, 1991.
[16] R. Nath, B. Rajagopalan, R. Ryker, Comput. Oper. Res. 24 (1997) 767–773.
[17] D.W. Marquardt, J. Soc. Ind. Appl. Math. 11 (1963) 431–441.
[18] A. Durán, J.M. Monteagudo, M. Mohedano, Appl. Catal. B: Environ. 65 (2006) 127–134.
[19] F.B. Li, X.Z. Li, X.M. Li, T.X. Liu, J. Dong, J. Colloid Int. Sci. 311 (2007) 481–490.